

# Single-ion scaling and unconventional Kondo behavior in the electrical resistivity of the $U_{1-x}Th_xPd_2Al_3$ system

R. P. Dickey, A. Amann, E. J. Freeman, M. C. de Andrade, and M. B. Maple

*Department of Physics and Institute for Pure and Applied Physical Sciences, University of California, San Diego, La Jolla, California 92093*

(Received 28 September 1999)

We report measurements of the temperature  $T$  dependence of the electrical resistivity  $\rho$  of the  $U_{1-x}Th_xPd_2Al_3$  system for thorium concentrations  $0.6 \leq x \leq 1.0$  in the temperature range  $0.02 \text{ K} \leq T \leq 300 \text{ K}$ . These measurements reveal an unconventional Kondo effect with an effective Kondo temperature  $T_K \approx 20 \text{ K}$ , which is independent of thorium concentration. The  $\rho(T)$  data below  $T_K$  scale with  $U$  concentration  $(1-x)$  and  $T_K$  in agreement with the scaling of  $C(T)$  and  $\chi(T)$  at low temperature that was previously established. Analysis of the data below  $20 \text{ K}$  indicates that the electrical resistivity in the non-Fermi-liquid regime saturates as a power law at the lowest temperatures with the form  $\rho(T) \sim 1 - a(T/T_K)^n$  with  $n \sim 1.5$ .

## I. INTRODUCTION

The last several years have seen increasing interest in a new class of materials that exhibit non-Fermi-liquid (NFL) behavior.<sup>1</sup> The NFL characteristics observed at low temperatures include a logarithmic or weak power-law divergence in the magnetic contribution to the specific heat and magnetic susceptibility and a nearly linear temperature dependence of the magnetic contribution to the electrical resistivity. New materials continue to be found whose physical properties deviate from the behavior predicted by conventional Fermi-liquid (FL) theory. However, there is still much to be learned from studying some of the first known materials in which NFL characteristics were found. A number of theoretical models have been developed,<sup>2-11</sup> but a conclusive picture has yet to emerge that describes all of the experimentally observed anomalous physical properties. In particular, it has been difficult to reconcile the available theoretical models of NFL behavior with the approximately linear temperature dependence of the electrical resistivity at low temperatures ( $T < 20 \text{ K}$ ).<sup>12-14</sup> One criticism of the studies on materials that display NFL behavior has been the limited temperature range over which the NFL behavior has been characterized. Many of the measurements of the physical properties of materials that exhibit NFL behavior have been performed only in the liquid-He regime above  $1 \text{ K}$ . Since NFL behavior typically occurs at temperatures  $T < 10-20 \text{ K}$ , the NFL behavior observed in these experiments extends over one decade in temperature at most. Recent experimental effort in our laboratory has been concentrated on extending the measurements down to temperatures of the order of  $100 \text{ mK}$  and lower.

The  $U_{1-x}Th_xPd_2Al_3$  system was first shown to exhibit NFL behavior several years ago.<sup>15</sup> Electrical resistivity  $\rho(T)$  measurements made at temperatures between  $1.2 \text{ K}$  and  $300 \text{ K}$  reveal an evolution from metallic behavior for a sample with no uranium ( $x=1$ ), through single-ion Kondo-like behavior for samples with  $0.95 \geq x > 0.4$ , to a coherent heavy-fermion state for  $x \leq 0.4$ , concomitant with antiferromagnetic ordering and superconductivity for  $x \leq 0.2$ . In particular,  $\rho(T)$  of samples with  $x=0.6$  and  $x=0.8$  show a nearly linear

increase with decreasing temperature below  $10 \text{ K}$  with no evidence of saturation down to the lowest measured temperature of  $1.2 \text{ K}$ . This linear increase is anomalous when compared to the resistivity of systems that exhibit a conventional single-ion Kondo effect and saturate quadratically at the lowest temperatures.<sup>16-18</sup> This quadratic saturation is due to quasiparticle scattering that can be described within a Fermi-liquid picture. The unconventional Kondo-like behavior found in the  $U_{1-x}Th_xPd_2Al_3$  system, among others, does not conform to Fermi-liquid theory and is thought to arise from a more complicated Kondo scenario.

Additional electrical resistivity measurements on the  $U_{1-x}Th_xPd_2Al_3$  system were made for temperatures down to  $250 \text{ mK}$  for samples with  $x=0.6, 0.8$ , and  $0.9$  and down to  $1 \text{ K}$  for a sample with  $x=0.95$ .<sup>19</sup> These data were found to deviate from a linear temperature dependence below roughly  $5 \text{ K}$ , and suggested that perhaps the NFL behavior is in the process of crossing over to Fermi-liquid behavior at low temperatures. A similar departure from linear behavior at low temperatures was found in recent measurements<sup>20</sup> of samples with  $x=0.4, 0.5, 0.6$ , and  $0.7$ . However, both specific heat and magnetic susceptibility measurements<sup>12,15,21</sup> show that NFL behavior persists down to the lowest temperatures measured (in some cases as low as  $100 \text{ mK}$ ). This discrepancy between the bulk thermodynamic and magnetic measurements and the transport measurements has not been resolved.

The work reported herein was motivated by two objectives. The first objective was to analyze the high-temperature ( $T > 10 \text{ K}$ ) electrical resistivity in order to obtain a better understanding of the Kondo behavior in this system. In particular, we wanted to determine whether the resistivity scaled with uranium concentration  $(1-x)$  as has been observed in the specific heat  $C(T)$  and magnetic susceptibility  $\chi(T)$  in previous measurements of the  $U_{1-x}Th_xPd_2Al_3$  system.<sup>15,19,21</sup> We were also interested in understanding the unusual uranium concentration dependence of the Kondo temperature determined from previous measurements.<sup>19</sup> The second objective was to measure the temperature dependence of the electrical resistivity at low temperatures ( $T < 2 \text{ K}$ ) over a wider range of thorium concentrations and a larger tempera-

ture range than was done previously. Here, we were interested in determining the temperature and thorium concentration  $x$  ranges over which the resistivity exhibits a NFL temperature dependence and identifying possible crossovers to FL behavior at very low temperatures. We were especially interested to see if NFL behavior persists to larger thorium concentrations than previously observed, which would imply that single-ion physics can account for the interesting NFL behavior observed.

## II. EXPERIMENTAL DETAILS

Details of the procedures used to prepare the polycrystalline  $U_{1-x}Th_xPd_2Al_3$  compounds studied in this work are described elsewhere.<sup>15</sup> The samples were cut into rectangular parallelepipeds with typical dimensions  $\sim 1 \times 1 \times 3$  mm<sup>3</sup> using an electrostatic discharge cutter. Low-resistance electrical contact to the samples was made by first sanding the surface of each sample to remove any oxide layer, and then evaporating gold through a mechanical mask covering each sample to create contact pads. 2 mil gold wires were then attached to the gold pads with silver epoxy (e.g., EPOTEK H2OE). This technique gives contact resistances typically of the order of 200 m $\Omega$ . After the leads were attached, the sample dimensions were measured using a Nikon MM-11 microscope.

The electrical resistivity measurements were made in a transverse geometry using two cryostats, an Oxford <sup>3</sup>He-<sup>4</sup>He dilution refrigerator in the temperature interval  $0.02$  K  $\leq T \leq 2$  K, and a Quantum Design PPMS in the interval  $1.7$  K  $\leq T \leq 300$  K. A Linear Research LR 700 low-dissipation four-wire ac resistance bridge operating at a frequency of 12 Hz was used for all of the low-temperature (dilution refrigerator) measurements. Resistance versus temperature sweeps were made by stabilizing the temperature against either germanium or RuO<sub>2</sub> thermometers, and then averaging the sample resistance for  $\sim 60$  sec. The sample resistance was measured using excitation currents between 3 mA at the highest temperatures and 100  $\mu$ A at the lowest temperatures. A superconducting magnet was used to apply a 500 Oe field for the low-temperature measurements of samples with  $0.9 \leq x \leq 1$  in order to quench the apparent filamentary superconductivity present in these materials. A future publication will discuss the superconductivity in this system in greater detail.

## III. RESULTS

Displayed in Fig. 1 are electrical resistivity  $\rho$  vs temperature  $T$  data for  $0.6 \leq x \leq 1$ . The sample dimensions were used to calculate the geometrical factor,  $A/l$ , where  $A$  is the cross-sectional area and  $l$  is the distance between voltage leads, which was used to convert the resistance data into resistivity data. Due to the large ( $\sim 10\%$ ) uncertainty in the geometrical factor caused by the deviation of the sample shape from a right parallelepiped, the uncertainty in the magnitude of the resistivity is  $\sim 10\%$  for all samples. In Fig. 2, the magnetic contribution to the electrical resistivity vs temperature  $T$  is plotted on a logarithmic temperature scale. Throughout this paper, we treat the uranium ions as magnetic “impurities” even though the uranium concentration is, in some samples,

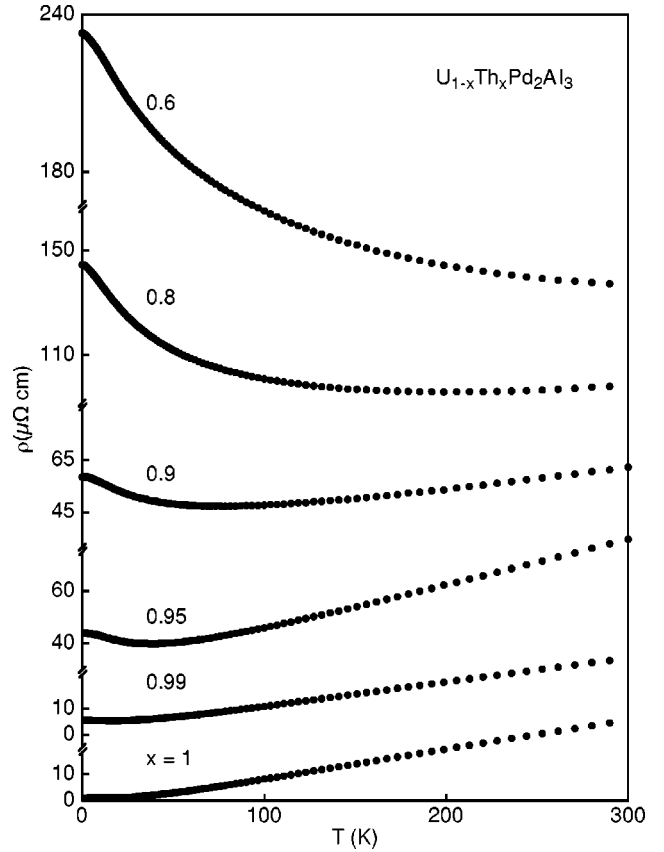


FIG. 1. Electrical resistivity  $\rho$  of  $U_{1-x}Th_xPd_2Al_3$  vs temperature  $T$  between 1.7 K and 300 K for thorium concentrations  $0.6 \leq x \leq 1$ . Note that the curves have been shifted vertically for clarity, but the relative scale for each curve is the same.

much larger than that of an impurity. For this reason, we refer to the magnetic contribution as a synonym for the contribution due to the uranium ions. The magnetic contribution to the resistivity was calculated by scaling the slope of the resistivity at high temperatures ( $T > 200$  K) for samples with  $x = 0.9, 0.95$ , and  $0.99$ , to match the slope of the resistivity at high temperatures in the  $x = 1$  compound. The resistivity data for samples with  $x = 0.6$  and  $0.8$  were not scaled due to the lack of a significant region of positive slope in these data at high temperatures. This scaling procedure normalizes the geometrical factor of each sample to the geometrical factor of the sample with  $x = 1$  so that the contribution to the resistivity from phonon scattering is more accurately eliminated. A numerical fit of the resistivity of the  $x = 1$  compound was then subtracted from the resistivity data for each uranium concentration to extract the magnetic contribution. It is evident from Fig. 2 that for  $x \geq 0.6$ , the samples exhibit a Kondo effect as determined by the logarithmic increase in the resistivity with decreasing temperature. An increase in the uranium concentration ( $1 - x$ ), and hence an increase in the number of Kondo scattering centers produces an anticipated increase in scattering (reflected in the increasing magnitude of  $\Delta\rho$  at low temperatures). It is apparent that the Kondo energy scale is roughly the same for all of the concentrations shown, since the deviation away from the  $-\ln T$  behavior occurs in the same temperature region for all of the samples.

In order to analyze the  $\rho(T)$  data in the NFL regime  $0.6 \leq x < 1$ , the magnetic contribution  $\Delta\rho(T)$  shown in Fig. 2 is

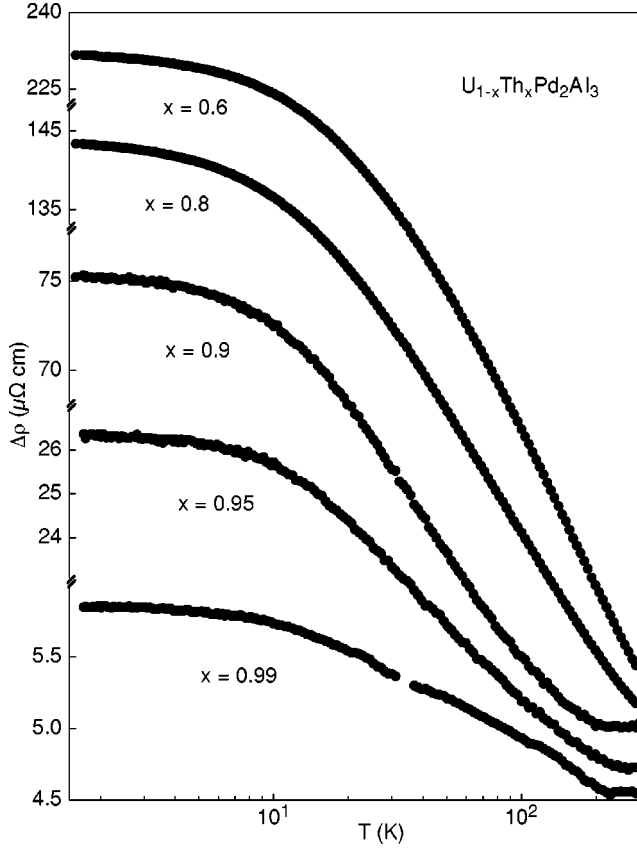


FIG. 2. Magnetic contribution of the electrical resistivity  $\Delta\rho$  of  $U_{1-x}Th_xPd_2Al_3$  vs temperature  $T$  on a logarithmic scale between 1.7 K and 300 K for thorium concentrations  $0.6 \leq x \leq 0.99$ . Note that the curves have been shifted vertically for clarity and the relative scale for each curve is quite different.

assumed to be composed of two parts,

$$\Delta\rho(T) = \Delta\rho_c + \Delta\rho_K(T), \quad (1)$$

where  $\Delta\rho_c$  is a temperature-independent term associated with potential scattering and  $\Delta\rho_K(T)$  is a temperature-dependent Kondo scattering term. The offset  $\Delta\rho_c$  was first subtracted from data for the magnetic contribution  $\Delta\rho(T)$  shown in Fig. 2 to extract  $\Delta\rho_K(T)$ . The  $\Delta\rho_K(T)$  data were then normalized by dividing by the extrapolated zero temperature value  $\Delta\rho_K(0)$ . The scaled  $\Delta\rho_K(T)/\Delta\rho_K(0)$  vs  $T$  data are shown in Fig. 3. Displayed in the inset of Fig. 3 are plots of the potential scattering contribution  $\Delta\rho_c$ , and the zero temperature value of the Kondo contribution  $\Delta\rho_K(0)$ , both of which initially increase linearly with the uranium concentration  $(1-x)$ . The overlap of the  $\Delta\rho_K(T)/\Delta\rho_K(0)$  vs  $T$  data for Th concentrations from  $0.6 \leq x \leq 0.99$  is indicative of single-ion scaling with a Kondo temperature ( $T_K$ ) that is constant over this range of Th concentrations. Here,  $T_K$  is defined as the temperature at which the resistivity has dropped to 80% of its zero temperature value, which is close to the temperature at which  $\Delta\rho_K(T)$  begins to deviate from a  $-\ln T$  behavior. From Fig. 3 we estimate  $T_K$  to be roughly 20 K for each of the  $\Delta\rho_K(T)/\Delta\rho_K(0)$  vs  $T$  curves shown in the figure. For the  $x=0.6$  and  $0.8$  samples, where it was not possible to scale the slopes of  $\rho(T)$  at high temperatures to

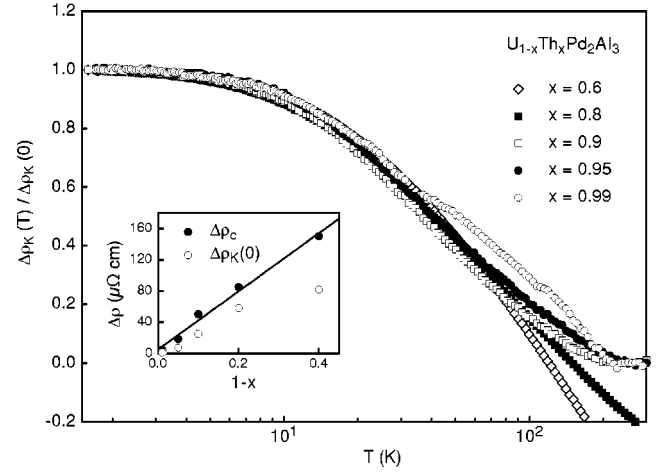


FIG. 3. Magnetic contribution to the electrical resistivity  $\Delta\rho_K$  vs temperature  $T$  for  $0.6 \leq x \leq 0.99$ , scaled by subtracting a potential scattering term  $\Delta\rho_c$  and then dividing through by the extrapolated zero temperature value of the Kondo scattering term  $\Delta\rho_K(0)$ . The inset shows the uranium concentration  $(1-x)$  dependence of the constant offset  $\Delta\rho_c$  and the zero temperature value of the Kondo contribution  $\Delta\rho_K(0)$ .

the  $\rho(T)$  curves for  $x=1$ , the constants  $\Delta\rho_c$  and  $\Delta\rho_K(0)$  were chosen to give the best collapse of the data.

As an example of the low-temperature results, Fig. 4 shows the temperature-dependent Kondo scattering contribution to the electrical resistivity for the sample with  $x=0.8$  in the temperature range  $0.02 \text{ K} \leq T \leq 30 \text{ K}$ . Assuming the Kondo scattering contribution to the resistivity follows the form

$$\Delta\rho_K(T) = \Delta\rho_K(0)[1 - a(T/T_K)^n] \quad (2)$$

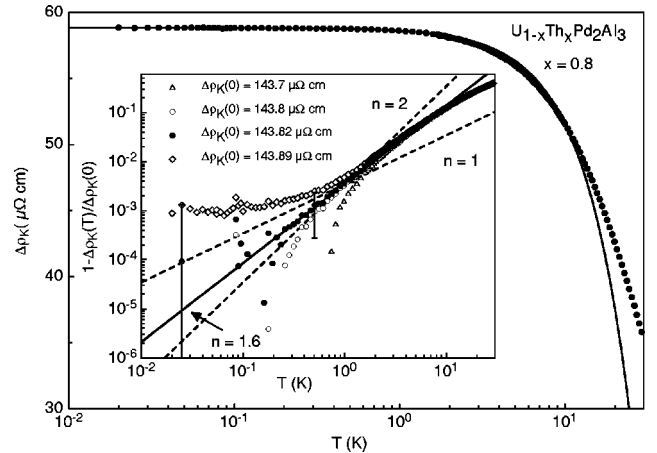


FIG. 4. Magnetic contribution to the electrical resistivity  $\Delta\rho_K$  vs temperature  $T$  for  $x=0.8$  in the temperature range  $0.02 \text{ K} \leq T \leq 30 \text{ K}$ . The solid line is a power-law fit of Eq. (2) to the low-temperature data between 0.02 K and 8 K. The inset shows the same data plotted as  $1 - \Delta\rho_K(T)/\Delta\rho_K(0)$  vs temperature  $T$  on a double logarithmic scale for several values of the residual resistivity  $\Delta\rho_K(0)$  indicated in the legend. All of the data overlap for  $T \geq 3 \text{ K}$ . The solid line is the same power-law fit as the main figure and its slope yields the value  $n=1.6$ . The two dashed lines are power-law fits with  $n=2$  and  $n=1$  as indicated.

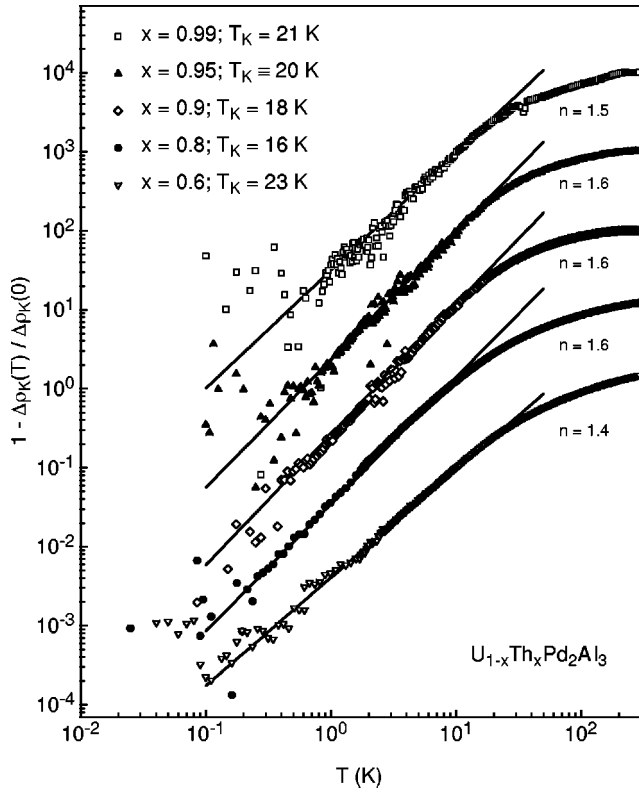


FIG. 5. Magnetic contribution to the electrical resistivity  $\Delta\rho_K$  vs temperature  $T$  plotted as  $1 - \Delta\rho_K(T)/\Delta\rho_K(0)$  on a double logarithmic scale for  $0.6 \leq x \leq 0.99$ . Note that each curve has been shifted vertically by one decade above the curve below it for the purpose of clarity, but the relative scale for each curve is the same. Values of  $T_K$  in the legend were calculated as described in the text.

at low temperatures, the solid line in the figure is a fit of this expression to the low-temperature data between 0.02 K and 8 K. Because of the difficulty in resolving the quality of the fit at the lowest temperatures in this type of plot, the inset shows the same data plotted as  $1 - \Delta\rho_K(T)/\Delta\rho_K(0)$  vs  $T$  on a double logarithmic scale for several values of the residual resistivity  $\Delta\rho_K(0)$ . The best value of  $\Delta\rho_K(0)$  is determined by plotting the data for several values of  $\Delta\rho_K(0)$  and choosing the one that gives the best approximation to a straight line at low temperatures. For the  $x=0.8$  sample, the solid circles represent the best value of  $\Delta\rho_K(0)$  using this criterion. The slope of a tangent to the data in the inset can be shown to equal the exponent  $n$ . The solid line is the same fit of Eq. (2) to the data as seen in the main figure, which results in a value of  $n=1.6$ . The increased scatter in the data at low temperatures is a result of the lower measuring currents used at low temperatures to reduce self-heating during the experiment. In fact, not all of the experimental data at low temperatures are shown in the inset. The scatter of the data results in some points that lie above the extrapolated value of  $\Delta\rho_K(0)$ , which are transformed into negative numbers in the calculation of  $1 - \Delta\rho_K(T)/\Delta\rho_K(0)$ . Due to the logarithmic y axis of the inset, these negative values are not plotted. The error bars in the inset reflect the standard deviation of the measurement of the resistance. Although the magnitude of the error bars does not increase very much at low temperatures, as the temperature gets smaller, the calculated value of  $1 - \Delta\rho_K(T)/\Delta\rho_K(0)$  becomes smaller until it is smaller than

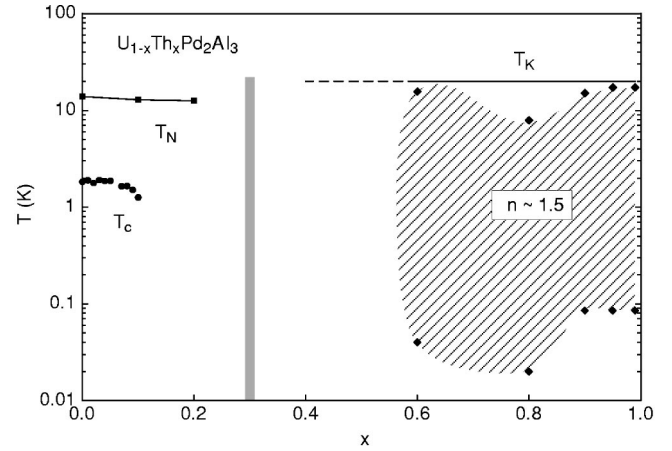


FIG. 6. Temperature  $T$  vs thorium concentration  $x$  phase diagram. The solid line illustrates the approximately constant Kondo temperature  $T_K$  and the shaded region denotes the low-temperature NFL regime where the resistivity scales as  $\rho(T) \sim 1 - a(T/T_K)^n$  with  $n \sim 1.5$ . The solid diamonds denote the high- and low-temperature limits of the fits shown in Fig. 5. The high-temperature limit of each fit is the temperature where the data begin to deviate from the fit shown in Fig. 5, whereas the low-temperature limit is the lowest temperature achieved in the measurement on the particular sample. Data from Ref. 19 for  $T_N$  and  $T_c$  are illustrated on the dilute thorium side of the phase diagram.

the uncertainty in the resistivity. Again, the logarithmic y axis causes error bars for these points to look anomalously large. However, it is quite clear that for  $T \geq 240$  mK the solid line provides a good description of the data. The dashed lines correspond to values of  $n=1$  and  $n=2$  as indicated in the inset. Although it is possible to fit the dashed curve with  $n=2$  to the data represented by open circles that has a slightly smaller value of  $\Delta\rho_K(0)$  than was chosen above, the data systematically deviate from this dashed curve below  $T=0.5$  K and the fit is satisfactory only up to  $\sim 2$  K. Therefore, the solid line representing  $n=1.6$  provides the best description of the data over the largest temperature range.

The low-temperature data for samples with  $0.6 \leq x \leq 0.99$  are shown in Fig. 5. The solid lines are fits of Eq. (2) to the data, and illustrate that the slope, and hence  $n$ , varies only slightly over this wide range of thorium concentration. The slope of each fit is indicated in the figure and varies between 1.4 and 1.6. For the largest thorium concentration,  $x=0.99$ , the fit provides a reasonable description of the data between 85 mK and 17 K. It is interesting to note that the high-temperature limit of the fit gradually decreases as the thorium concentration decreases down to  $x=0.8$ , and then increases to almost 16 K for  $x=0.6$ . The low-temperature limit of each fit was taken to be the lowest temperature for which a data point was measured. To calculate values of  $T_K$  from the low-temperature fits, we arbitrarily fixed  $T_K=20$  K for the  $x=0.95$  sample, which seems appropriate in light of the high-temperature data in Fig. 3, which allowed us to determine the value of  $a=0.3$ . Using this value for  $a$ , the values of  $T_K$  for the other thorium concentrations were calculated and are displayed in the legend of Fig. 5.

The main results of this work are summarized in the temperature vs thorium concentration  $x$  phase diagram shown in Fig. 6. Non-Fermi-liquid behavior is found for temperatures

below  $T_K$  on the dilute uranium side of the phase diagram. The shaded region indicates the temperature interval over which the resistivity scales as  $\rho(T) \sim 1 - a(T/T_K)^n$  with  $n \sim 1.5$ . The high- and low-temperature limits of the fits in Fig. 5 are indicated by solid diamonds on the perimeter of the shaded region. The high-temperature limit of each fit is the temperature where the data began to deviate from the fit shown in Fig. 5, whereas, the low-temperature limit is the lowest temperature achieved in the measurement of the particular sample. The Kondo temperature is denoted by the solid line above the NFL regime, and is fixed in temperature across the phase diagram. On the dilute thorium side of the phase diagram, antiferromagnetic ordering occurs for  $x \leq 0.2$  and superconductivity for  $x \leq 0.1$ .

#### IV. DISCUSSION

Single-ion scaling has been observed in several NFL systems to date.<sup>22</sup> If a single-ion mechanism, like a multichannel Kondo effect, is responsible for the NFL behavior observed in the  $U_{1-x}Th_xPd_2Al_3$  system, then there are a number of clues that one expects to find in experimental measurements. The most important evidence would be scaling of all of the physical properties with the concentration of the magnetic species (i.e., uranium) over a wide range of concentrations, including very low concentrations. This evidence would suggest that NFL behavior persists in the single-ion limit, and since this behavior is independent of concentration, intersite correlations do not play an appreciable role in the physics of these systems. Based on this expectation, the scaling of the data in Fig. 3 implies that a single-ion picture is the appropriate way to think about the scattering processes that lead to the logarithmic increase in the resistivity with decreasing temperature. This conclusion is in agreement with the strong evidence for scaling from previous low-temperature specific heat<sup>12,19,21</sup> and magnetic susceptibility measurements<sup>12,15</sup> in the concentration range  $0.4 \leq x \leq 0.95$ . Above roughly 50 K, the quality of the scaling in Fig. 3 worsens. This is not altogether unanticipated, since changes in the phonon spectrum are expected to become more important at higher uranium concentrations at high temperatures. The deviations seen might also be a result of departures from Matthiessen's rule that historically has made the saturating Kondo scattering contribution at temperatures far above  $T_K$  difficult to observe.<sup>23</sup> In addition, there is more noise in the data for the  $x=0.99$  sample because of its comparatively smaller resistance. The fact that the data for samples with  $x=0.6$  and  $x=0.8$  do not saturate to a constant at high temperatures (i.e., at 300 K) may indicate that at these concentrations, intersite correlations are beginning to be significant.

The offset  $\Delta\rho_c$ , which is presumed to be associated with potential scattering, is expected to be proportional to the number of scattering centers, and hence the uranium concentration  $(1-x)$ . The extrapolated zero temperature value of the Kondo scattering contribution  $\Delta\rho_K(0)$  is equivalent to the unitarity scattering limit in a material that exhibits a conventional Kondo effect and should also increase in proportion to the uranium concentration  $(1-x)$ . The unitarity scattering limit for  $5f$  electrons is given by<sup>24</sup>

$$\rho_{fu} = (2l+1) \frac{2m^*c}{\pi n \hbar e^2 N(E_F)}, \quad (3)$$

where  $l$  is the  $f$ -electron angular momentum quantum number ( $l=3$  in this case),  $m^*$  is the effective mass of the conduction electrons,  $c$  is the impurity concentration,  $n$  is the conduction electron density,  $\hbar$  is Planck's constant divided by  $2\pi$ ,  $e$  is the charge of the electron, and  $N(E_F)$  is the density of states in the host material at the Fermi energy. A simple calculation for the  $U_{1-x}Th_xPd_2Al_3$  system based on an estimated value of the Fermi wave vector and the experimental electronic specific heat coefficient ( $\gamma$ ) gives, for instance, for  $x=0.9$ , a value of  $23 \mu\Omega \text{ cm}$ . This value is in good agreement with the experimental results shown in the inset to Fig. 3 where we estimate  $\Delta\rho_K(0) \approx 25 \mu\Omega \text{ cm}$  for the  $x=0.9$  sample. This agreement reinforces the idea that the low-temperature properties are the result of single-ion Kondo-like physics.

Another piece of evidence pointing towards a single-ion mechanism would be a sensible energy scale that characterizes the single-ion behavior. In conventional systems (which exhibit Fermi-liquid behavior) that show Kondo phenomena, this energy scale is the Kondo temperature  $T_K$ . The Kondo temperature depends exponentially on the exchange interaction parameter  $J$  as

$$T_K \sim T_F \exp[-1/N(E_F)J], \quad (4)$$

where  $T_F$  is the Fermi temperature,  $N(E_F)$  is the density of states at the Fermi level, and  $J \sim -\langle V_{kf}^2 \rangle / e_{5f}$ , where  $V_{kf}$  is the hybridization matrix element between the conduction electrons and the  $5f$  electrons, and  $e_{5f}$  is the binding energy of the  $5f$  electrons. Our result, as seen in Fig. 6, suggests that  $T_K$  is constant across the dilute side of the phase diagram. A change in  $T_K$  is not expected since in this system tetravalent thorium is replaced with tetravalent uranium and, hence, the electron concentration and  $5f$  binding energy should remain the same. This is a modification of the preliminary phase diagram<sup>19</sup> that suggested that  $T_K$  increased with increasing  $x$ . Strong evidence that uranium in  $U_{1-x}Th_xPd_2Al_3$  is tetravalent was provided by the work of Geibel *et al.*,<sup>25</sup> who found that tetravalent substitutions in  $UPd_2Al_3$  (including  $Th^{4+}$ ) suppress the Néel temperature  $T_N$  and superconducting transition temperature  $T_c$  with increasing substituent concentration at a much lower rate than trivalent substitutions such as  $Y^{3+}$ . This contrast was confirmed in recent work<sup>14</sup> on the  $Y_{1-x}U_xPd_2Al_3$  system. On the other hand, a rapid increase of  $T_K$  with decreasing uranium concentration has been observed in the  $Y_{1-x}U_xPd_3$  system.<sup>12</sup> In  $Y_{1-x}U_xPd_3$ , the substitution of trivalent uranium for trivalent yttrium increases the Fermi level and, in turn  $e_{5f}$ , which causes  $T_K$  to decrease with increasing uranium concentration, assuming that the host density of states in  $YPd_3$  and the hybridization are approximately constant.

Finally, one of the most interesting aspects of this work concerns the temperature dependence of the electrical resistivity at very low temperatures. Our experiments indicate that the NFL behavior in the  $U_{1-x}Th_xPd_2Al_3$  system does, in fact, persist down to the lowest temperatures measured, but has a different temperature dependence than previously reported. The electrical resistivity is best described by a power

law [Eq. (2)] with  $n \sim 1.5$  over a range that extends more than two decades in temperature and persists to the highest thorium concentration ( $x = 0.99$ ) measured to date. Previous measurements suggested that the resistivity increases linearly with decreasing temperature below 10 K and then levels off below roughly 5 K. This apparent crossover to Fermi-liquid behavior was taken at face value despite the persistence of NFL behavior in the magnetic susceptibility and specific heat measurements to much lower temperatures.<sup>12</sup> We now believe that the low-temperature saturation of the resistivity previously observed is an artifact due to filamentary superconductivity. Application of a 500 Oe magnetic field quenched the superconductivity, allowing the resistivity to be traced to lower temperatures. The absence of magnetoresistance was established by increasing the value of the applied field to 1 kOe and observing no change in the resistivity trace.

The power-law behavior of  $\rho(T)$  with an exponent  $n = 1.5$  observed for  $U_{1-x}Th_xPd_2Al_3$  is quite different from that expected for the two-channel spin-1/2 Kondo model<sup>26</sup> where  $\rho(T)$  is predicted to saturate with a power-law exponent  $n = 0.5$ , as well as the linear  $T$  dependence that has been observed in many NFL materials.<sup>19,22</sup> It is interesting to note that the  $n \sim 1.5$  power-law behavior for  $\rho(T)$  of  $U_{1-x}Th_xPd_2Al_3$  observed here is intermediate between the value  $n \approx 1$  found for other NFL materials, and the value of  $n = 2$  expected for an  $f$ -electron Fermi-liquid material. It is not clear whether this implies that the  $U_{1-x}Th_xPd_2Al_3$  system is somehow “closer” to being a Fermi liquid than a system like  $Y_{1-x}U_xPd_3$ .

In a recent paper<sup>27</sup> it has been suggested that the NFL behavior of the  $U_{1-x}Th_xPd_2Al_3$  system, among others, can be described within the context of a Griffiths phase model based on low-temperature specific heat and magnetic susceptibility measurements. Since there are no predictions for the  $T$  dependence of the electrical resistivity in the Griffiths phase model, we are unable to compare this model to our experimental results at this time. It is interesting that power-law behavior of  $\rho(T)$  with  $n \sim 1.5$  is similar to that observed in the stoichiometric compounds  $CePd_2Si_2$  and  $CeIn_3$  at pressures near the critical pressure at which the Néel temperature

$T_N$  of these antiferromagnetic compounds vanishes and superconductivity appears.<sup>28</sup> In that work, power-law behavior of  $\rho(T)$  with  $n \sim 1.5$  is attributed to antiferromagnetic spin fluctuations in a three-dimensional antiferromagnet within the framework of spin-fluctuation theory, originally developed for itinerant  $d$ -electron systems. However, it is difficult to see how such a spin fluctuation theory would be applicable to the  $U_{1-x}Th_xPd_2Al_3$  system in view of the difficulty in identifying a critical concentration where  $T_N$  vanishes (antiferromagnetic quantum critical point) and the scaling of  $\rho(T)$  with  $(1-x)$  and  $T_K$  over such a large range of  $U$  concentration  $(1-x)$ .

## V. CONCLUSION

We have made a detailed investigation of the low-temperature electrical resistivity in the  $U_{1-x}Th_xPd_2Al_3$  system over the range of thorium concentrations  $0.6 \leq x \leq 1$ . We observed an unconventional Kondo effect with a characteristic scaling temperature  $T_K \approx 20$  K. The electrical resistivity data were found to scale with uranium concentration, reinforcing the idea that a single-ion picture best describes the physics of this system. The temperature vs thorium concentration  $x$  phase diagram exhibits a large region at low temperatures where the temperature dependence of the electrical resistivity exhibits power-law behavior with an exponent  $n \approx 1.5$ . Although it is currently not clear how this power-law behavior arises, it is evident that this behavior persists to low uranium concentrations, and hence is most likely the result of single-ion physics.

## ACKNOWLEDGMENTS

We acknowledge illuminating discussions with D. L. Cox and D. A. Gajewski. The research was supported by the National Science Foundation under Grant No. DMR-97-05454, the U.S. Department of Energy under Grant No. DE-FG03-86ER-45230, and by the UC CLC LA 95-0519-BM. In addition, equipment used in the research at UCSD was provided by the National Science Foundation under Grant No. DMR-94-03836.

<sup>1</sup>See, for instance, *Proceedings of the Conference on Non-Fermi Liquid Behavior in Metals, Santa Barbara, 1996*, edited by P. Coleman, M. B. Maple, and A. Millis [J. Phys.: Condens. Matter **8** (1996)].

<sup>2</sup>P. Schlottman and P. D. Sacramento, Adv. Phys. **42**, 641 (1993).

<sup>3</sup>D. L. Cox, Phys. Rev. Lett. **59**, 1240 (1987).

<sup>4</sup>T. Moriya, *Spin Fluctuations in Itinerant Electron Magnetism* (Springer, Berlin, 1985).

<sup>5</sup>A. J. Millis, Phys. Rev. B **48**, 7183 (1993).

<sup>6</sup>A. M. Tsvelik and M. Reizer, Phys. Rev. B **48**, 9887 (1993).

<sup>7</sup>S. Sachdev, N. Read, and R. Oppermann, Phys. Rev. B **52**, 10 286 (1995).

<sup>8</sup>O. O. Bernal, D. E. MacLaughlin, H. G. Lukefahr, and B. Andraka, Phys. Rev. Lett. **75**, 2023 (1995).

<sup>9</sup>E. Miranda, V. Dobrosavljević, and G. Kotliar, J. Phys.: Condens. Matter **8**, 9871 (1996).

<sup>10</sup>S. H. Liu, Physica B **240**, 49 (1997).

<sup>11</sup>A. H. Castro Neto, G. Castilla, and B. A. Jones, Phys. Rev. Lett. **81**, 3531 (1998).

<sup>12</sup>M. B. Maple, C. L. Seaman, D. A. Gajewski, Y. Dalichaouch, V. B. Barbeta, M. C. de Andrade, H. A. Mook, H. G. Lukefahr, O. O. Bernal, and D. E. MacLaughlin, J. Low Temp. Phys. **95**, 225 (1994).

<sup>13</sup>R. P. Dickey, M. C. de Andrade, J. Herrmann, M. B. Maple, F. G. Aliev, and R. Villar, Phys. Rev. B **56**, 11 169 (1997).

<sup>14</sup>E. J. Freeman, M. C. de Andrade, R. P. Dickey, N. R. Dilley, and M. B. Maple, Phys. Rev. B **58**, 16 027 (1998).

<sup>15</sup>Y. Dalichaouch and M. B. Maple, Physica B **199&200**, 176 (1994).

<sup>16</sup>A. D. Caplin and C. Rizzuto, Phys. Rev. Lett. **21**, 746 (1968).

<sup>17</sup>C. Rizzuto, E. Babić, and A. M. Stewart, J. Phys. F **3**, 825 (1973).

<sup>18</sup>M. B. Maple, J. G. Huber, B. R. Coles, and A. C. Lawson, J. Low

- Temp. Phys. **3**, 137 (1970).
- <sup>19</sup>M. B. Maple, M. C. de Andrade, J. Herrmann, Y. Dalichaouch, D. A. Gajewski, C. L. Seaman, R. Chau, R. Movshovich, M. C. Aronson, and R. Osborn, J. Low Temp. Phys. **99**, 223 (1995).
- <sup>20</sup>P. de V. du Plessis, A. M. Strydom, R. Troć, T. Cichorek, C. Marucha, and R. P. Gers, J. Phys.: Condens. Matter **11**, 9775 (1999).
- <sup>21</sup>M. B. Maple, M. C. de Andrade, J. Herrmann, S. H. Han, R. Movshovich, D. A. Gajewski, and R. Chau, Physica C **263**, 490 (1996).
- <sup>22</sup>M. B. Maple, R. P. Dickey, J. Herrmann, M. C. de Andrade, E. J. Freeman, D. A. Gajewski, and R. Chau, J. Phys.: Condens. Matter **8**, 9773 (1996).
- <sup>23</sup>J. W. Loram, T. E. Whall, and P. J. Ford, Phys. Rev. B **2**, 857 (1970).
- <sup>24</sup>M. D. Daybell, in *Magnetism*, edited by G. T. Rado and H. Suhl (Academic, New York, 1973), Vol. 5, p. 131.
- <sup>25</sup>C. Geibel, C. Schank, F. Jährling, B. Buschinger, A. Grauel, T. Lühmann, P. Gegenwart, R. Helfrich, P. H. P. Reinders, and F. Steglich, Physica B **199&200**, 128 (1994).
- <sup>26</sup>A. W. W. Ludwig and I. Affleck, Phys. Rev. Lett. **67**, 3160 (1991).
- <sup>27</sup>M. C. de Andrade, R. Chau, R. P. Dickey, N. R. Dilley, E. J. Freeman, D. A. Gajewski, M. B. Maple, R. Movshovich, A. H. Castro Neto, G. Castilla, and B. A. Jones, Phys. Rev. Lett. **81**, 5620 (1998).
- <sup>28</sup>S. R. Julian, F. V. Carter, F. M. Grosche, R. K. W. Haselwimmer, S. J. Lister, N. D. Mathur, G. J. McMullan, C. Pfleiderer, S. S. Saxena, I. R. Walker, N. J. W. Wilson, and G. G. Lonzarich, J. Magn. Magn. Mater. **177–181**, 265 (1998).